Flexural Behavior of Corroded Steel Fiber Reinforced Concrete Beams with Variable Fiber Contents

Seihak Heang[1,*] Pornpen Limpaninlachat[2] Punyawut Jiradilok[3] Thatchavee Leelawat[4] Withit Pansuk[5]

[1,2,4] Department of Civil and Environmental Engineering, Faculty of Engineering, Mahidol University, Nakhon Pathom, THAILAND

[3] Department of Civil Engineering, Faculty of Engineering, Kasetsart University, THAILAND

[5] Center of Excellence in Innovative Construction Materials, Department of Civil Engineering, Faculty of Engineering, Chulalongkorn University, Bangkok, THAILAND

**Corresponding author; E-mail address: seihak.hea@student.mahidol.ac.th*

Abstract

Steel fiber reinforced concrete (SFRC) is introduced to the construction due to the capability of the load enhancement and restraining the crack opening, which leads to higher structural performance and longer durability. The main purpose of this study was to study the effectiveness of steel fiber contents in SFRC beams under corrosion to the crack propagation and flexural loading capacity. Four SFRC beams were fabricated with same dimension of 100 x 200 x 1400 mm including 4 deformed bars with diameter of 12mm. Moreover, 6mm stirrups were reinforced to avoid shear failure. The contents of mil-cut steel fiber varied from 0%, 0.5%, 1.0% and 1.5%. All specimens were accelerated by the impressive current (ICT) method within 19 days. Crack width of the specimens were measured and recorded to analyze the crack propagation during the ICT method. Specimens were subjected to the four-point bending test for investigating the capacity, deflection, and failure pattern. The results showed that the increase of fiber contents could reduce the overall crack and lead to the higher yield loading of SFRC beams as well.

Keywords Steel Fiber Reinforced Concrete, Steel Corrosion, Flexural Performance, Crack Width, Failure Pattern

1. Introduction

Reinforced concrete is commonly used due to its low construction cost, durability, and the ability to cast into any shape of the construction elements. In today's world of construction, structures have been issued with many serious deteriorations against the environment problem where they are located. Among the problems, corrosion of steel rebar is the most harmful and costly mechanism which should be considered because it will affect the service life and lead to structure failure. There is $150 billion of corrosion damage on their interstate highway bridges in America due to deicing and sea salt-induced corrosion. In a Transportation Research Board report on the costs of deicing [1], the annual cost of bridge deck repairs was estimated to be $50–200 million. For substructures and other components required $100 million a year and a further $50–150 million a year for multi-story parks.

When crack in the concrete initiates and widens, it allows the chloride getting in the concrete faster and finally leads to the corrosion of rebar. Therefore, steel fiber randomly distributed in the concrete known as steel fiber reinforced concrete (SFRC) was introduced in the construction field to delay the crack widening effectively in the concrete and enhance the flexural performance. SFRC is composed of cement, water, fine, coarse aggregates, and discrete steel fibers. Concrete is a brittle material with a poor strain capacity, particularly when subjected to tensile stress. The fibers in the concrete actively participate in arresting the extension of the microcracks existing in the interfacial transition zone, their widening, and their further progress into the mortar matrix after the formation of a first crack in the concrete. The addition of randomly distributed fibres to a structural element generally improves the post-cracking tensile capacity and energy absorption performance of the cementitious matrix [2].

Up to date, steel fiber has been adopted to enhance the flexural performance of the concrete and control the crack as a new structural material. Many researchers [3-10] conducted

experiments and numerical analysis to understand the performance of steel fiber in corrosion condition and they show excellent performance. However, the research carried out more serious damage of corrosion degree with full scale beam has not been studied. Accordingly, the flexural testing of full scale SFRC beams under severe corrosion has been conducted to determine the effect of steel fiber to the corrosive crack propagation and flexural behavior. A serious damage due to corrosion was accelerated to four SFRC beams with variable fiber content within 19 days under high current of 500 $\mu A/cm^2$. Four SFRC beams were fabricated with a dimension of 100 x 200 x 1400mm reinforced by 2 deformed bars with diameter of 12mm for each top and bottom reinforcement. The specimens were cast by distributed randomly of various steel fiber content from 0%, 0.5%, 1.0% and 1.5%. All specimens were then subjected to a four-point bending test to observe the flexural performance of each beam. Flexural behavior and failure pattern of the specimens were study and discuss in the follow section.

2. Methodology

2.1 Experimental parameters

Four SFRC beams were fabricated with the same material and dimension except the volume fraction of the steel fiber, which were 0%, 0.5%, 1.0% and 1.5% of concrete volume. The specimens were fabricated with 40 MPa compressive strength concrete. All specimens were induced by the chloride by impressive current (ICT) method over the same duration of 19 days. Table 1 illustrates the specimen's ID and varied parameters.

Table 1 Experimental parameters.

No	ID	Fiber	Corrosion period
1	C19F0	0%	19 days
2	C19F0.5	0.5%	
3	C19F1.0	1.0%	
4	C19F1.5	1.5%	

**Note: Specimen's name is denoted as the immersion date to achieve the corrosion for 19 days and the fiber volume fraction in the SFRC beam.*

2.2 Experimental details

All SFRC beams had dimensions of 200mm x 150mm x 1400 mm with a covering of 25mm and effective depth 163mm. Four longitudinal deformed bars with 12mm diameter were reinforced for both top and bottom reinforcements. The 6mm stirrups with 100mm spacing were uniformly applied in all specimens to prevent the shear failure. Moreover, the compression bars and stirrups were epoxy-coated to prevent the formation of local pitting corrosion, which could lead to shear failure. All parts of the beam were designed in accordance with ACI 318-19 [11] to achieve ductile flexural failure. The details of SFRC beam specimens are presented in Fig. 1.

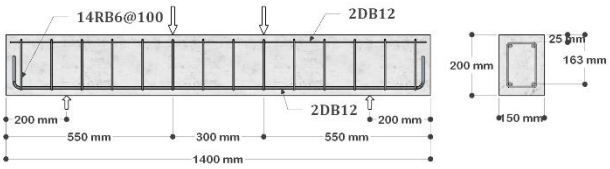

Fig. 1 Details of the section of specimens

2.3 Materials

The targeted cylindrical compressive strength was 40 MPa in this study. As a result, the mixed proportion of SFRC beams had a water to cement ratio of 0.4. Each mix consisted of Ordinary Portland Cement Type I, river sand size of less than 1 mm, coarse aggregate with maximum aggregate size of 20 mm and variable amount of steel fibers. In addition, the superplasticizer was used 1.0% to weight of cement in the mix proportion to improve the workability for casting. The mixed proportions of SFRC are shown in Table 2.

The mill-cut steel fiber with hooked ends as shown in Fig 2 was used in this study. It had a length of 32 mm and a width of 2.6 mm. The properties of mill-cut steel fiber are tabulated in Table 3.

For the steel reinforced in the concrete specimens, two deformed bars with 12 mm diameter were applied for each top and bottom longitudinal bar. These longitudinal bars has the yield strength at least 390 MPa conformed to TIS 24-2003. The round bars with 6 mm diameter with the yield strength at least 240 MPa according to TIS 20-2000 were used as stirrup.

Table 2 Mix proportion of SFRC beams.

Cement (kg)	Sand (kg)	Aggregate (kg)	Water (kg)	Steel Fiber (%)	Superplasticizer (%)
445	666	1126	178	0-1.5	1.0

Table 3 The properties of mill-cut steel fiber.

Length, l (mm)	Width, d (mm)	Aspect ratio l/d	Tensile Strength (MPa)	Specific gravity
32.0 ± 2.0	2.6 ± 1.2	35-45	≥ 700	8.9

Fig. 2 Mill-cut steel fibers with hooked ends [3]

2.4 Fabrication procedure

The casting procedure was conducted under conventional laboratory conditions at room temperature. The process of casting began with the mixing of cement and aggregates, followed by the addition of water with superplasticizer, and eventually the distributed addition of mill-cut steel fibers. Due to attain the uniformly dispersed steel fiber, the additional casting time was required comparing to ordinary concrete. The mixing of SFRC was cast into the prepared steel molds; the high frequency concrete vibrator was used for improving the rheology into the molds. After leveling surface, all specimens were cured for 28 days under controlled moisture condition by sack covering and watering 3 times each day.

2.5 Experimental setup

2.5.1 Corrosion acceleration process

After complete curing procedure, the specimens were induced corrosion. The impressed current technique (ICT) was used to accelerated corrosion, so that, the corrosive specimens could be completed within a reasonable amount of time. Corrosion is induced by applying an electrochemical potential between the steel reinforcement and a cathode. These beams were immersed in a 3% sodium chloride solution at a depth covered the tensile steel bars. This condition ensures that the beam is in a saturated state by admitting both oxygen and moisture. A water tank was constructed for the ICT facility, which is seen in Fig 3. The steel bars were connected to the positive terminal of the DC power supply, while the negative terminal was connected to a parallel-positioned stainless-steel bar. In addition, to confirm the constant current induced to the specimens, the multimeter was used for measuring the current during the tests as displayed in Fig. 4.

Fig. 3 Acceleration corrosion set up.

Fig. 4 Measuring the current by a multimeter.

The current density was maintained at 500μA/cm^2 for all specimens. The time for achieving the corrosive levels was calculated according to Faraday's law [12] in Equation 1.

$$\Delta_m = \frac{MIt}{zF} \quad (1)$$

Where;

M is atomic weight of metal (56g for Fe);

I is current (amperes);

t is time (second);

z is ionic charge (equal to 2);

F is Faraday Constant (equal to 96500 C/mol).

To achieve the current density, this formula [13] was calculated:

$$I = \frac{i_{applied}}{A} \quad (2)$$

Where;

I is current density ($\mu A/cm^2$);

$i_{applied}$ is the DC current applied (μA);

A is surface of the rebar (cm^2).

2.5.2 Crack measurement

To collect the crack propagation during the corrosive induction, all specimens were measured the crack width by using crack scale (Fig. 5) at the interval time. Corrosion of the rebar in the specimens will expand and finally push the concrete surface out and leave the crack along the rebar alignment. During the corrosion acceleration process, cracks were investigated every three days to see the crack width and the crack propagation for studying the effect of steel fiber bridging the crack. The crack width was observed on three sides (bottom, right and left) of the beams around the level of longitudinal reinforcement. The location for tracking the crack was divided into every 100 mm along the beams as displayed in Fig. 6. As a result, the recorded crack widths will be compared between specimens with different volumes of steel fibers.

Fig. 5 Crack measurement tool

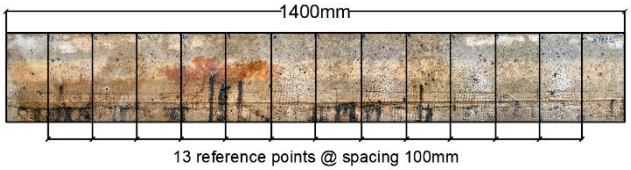

Fig. 6 Referenced point for tracking crack width

2.5.3 Four-point loading test setup

All specimens were subjected to the four-point bending test to investigate their flexural capacities and failure pattern influenced by the various fiber contents. The experimental set up is shown in Fig. 7. In every loading test, the SFRC beam was tested with symmetrical span length of 350 mm. The loading plates were spanned from the center of beam equal to 150 mm. Several measurements were attached on the beam to observe flexural behavior. Three strain gauges attached on the surface of SFRC beam; at the middle top, at the level of tensile reinforcement at the middle of the beam, and at the shear span, for determining the real strains with load increasing at compression zone, tension zone, and shear span area. Four Linear Variable Differential Transducers (LVDTs) were also installed at middle (2 LVDTs) and each side of supporting plates for calculating the relative displacement. In addition, the cameras were set up to capture the failure pattern every 5 kN of loading test. The machine increased the load until the failure of specimen, and all data were recorded by using data logger for analysis and discussion in the next step.

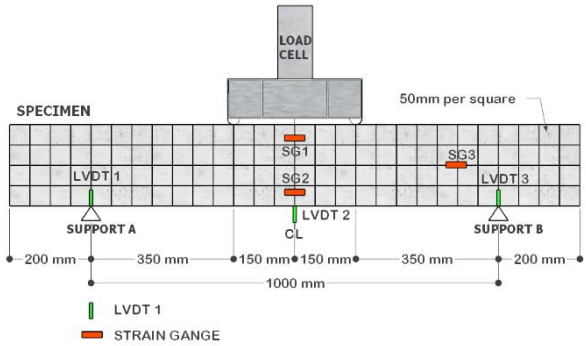

Fig. 7 Four-point flexural beam test

3. Results and discussion

3.1 Crack propagation

During the corrosion acceleration period, all specimens were monitored and recorded the crack development on the referenced points every 3 days. However, the crack was able to be observed since the 13th day. Consequently, corrosion cracks were found and recorded along the tensile longitudinal bars at the 13th, 16th and 19th day (the last date of induced corrosion).

Figure 8 shows the example of crack propagation in RC beam without steel fiber (C19F0) which were measured from 13th day,

16th day and 19th day of the corrosion acceleration period. The cracks formed along the steel rebar of the beam and the width increased larger due to the ICT process and the absence of steel fiber. The cracks were measured on the 13 reference points from all three sides of the beam. After the 19th day of corrosion acceleration period, the crack data was recorded and analyzed.

The experiments show that beam C19F0 has a maximum crack width of 0.4 mm and the overall crack width from all three sides of the beam is 0.23 mm which was higher than other SFRC beam. The crack significantly increases the width along the longitudinal rebar while SFRC form more crack point but in smaller crack width. This is proof that the effectiveness of steel fiber reduces the crack width effectively compared to normal RC beam. At the bottom side of the beam, the crack forms a long stirrup randomly and increases the width due to the corrosion time.

Figure 10 shows the average crack widths from three sides of the beam (left, right, bottom) from each recording date. The results from the beams with various amounts of fiber volume were compared. By considering maximum crack width at the last date, the crack widths significantly reduced from 0.20mm to 0.17mm for RC beam (C19F0) to the 1.5% SFRC beam. The tendency of crack width reducing with higher amount of fiber volume had shown in every recording date which performed the high performance to restrain the crack opening with the more fiber volume in the beam. In Fig. 10, all average results of crack width were plotted to observe the effect of fiber volume to the crack propagation. The cracks propagation during the corrosion acceleration period was reduced with higher fiber volume. Especially, the significant reduction of crack opening presented in the highest amount of fiber beam. It is noticed that the steel fiber works perfectly to reduce the crack development compared to RC beam.

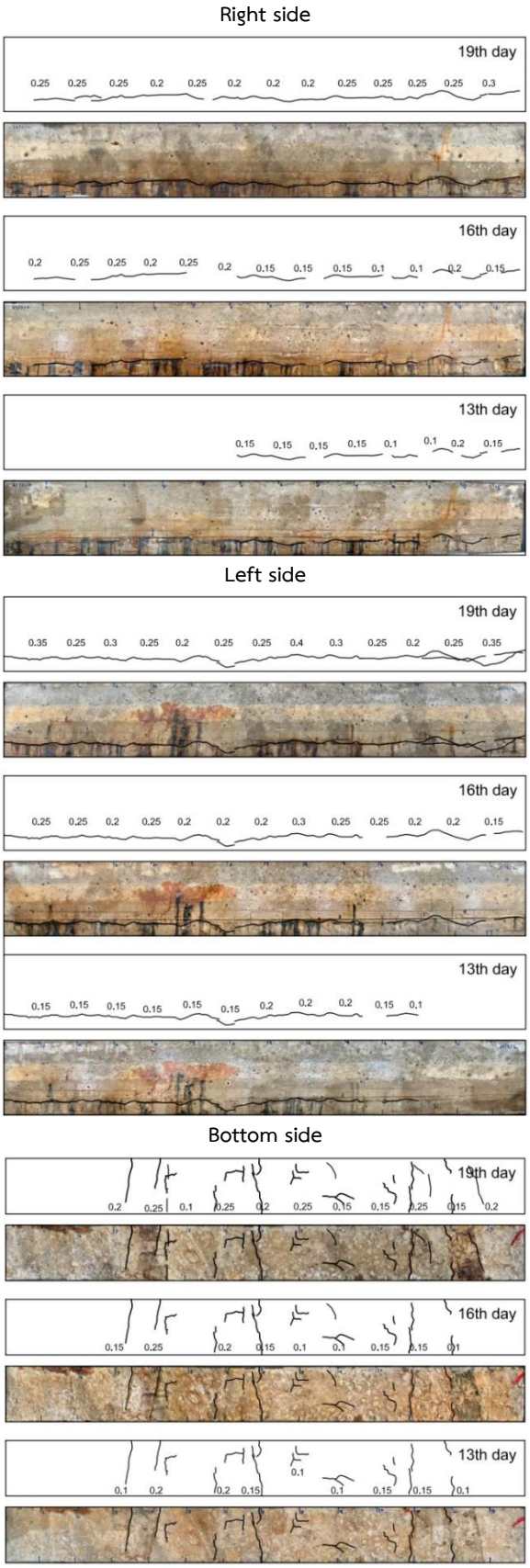

Fig. 8 Crack development of C19F0 beam during last three date (13th, 16th and 19th day)

Figure 9 shows the comparison of crack between SFRC beam (C19F0.5-R) with RC beam (C19F0-L). After the corrosion acceleration of the beam, many cracks form along the rebar on SFRC beam but in small width due to crack control of steel fiber. Meanwhile, RC beam allows the crack to increase the width wider in the same crack point.

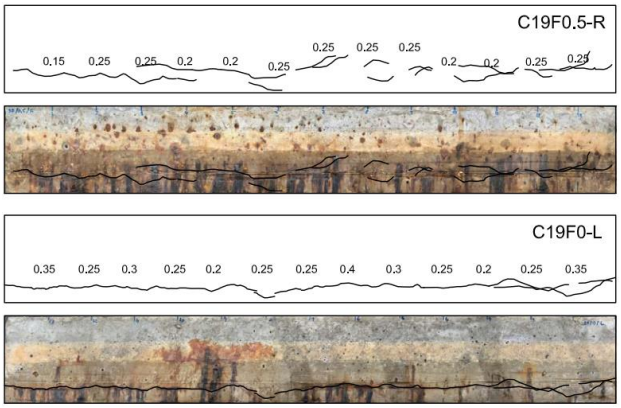

Fig. 9 Crack comparison between SFRC beam (C19F0.5-R) and RC beam (C19F0-L)

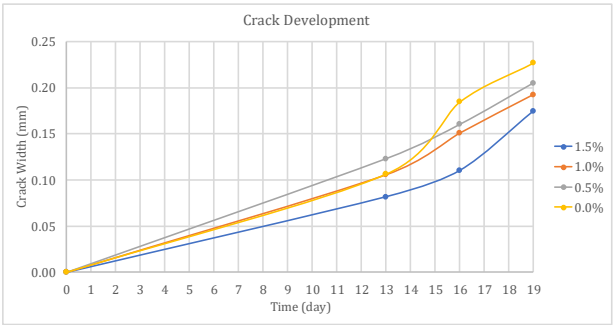

Fig. 10 Crack propagation of all beams

3.2 Flexural test result of the beams

Figure 11 to 14 show the load—deflection curves, which the resemble failure pattern are observed. The flexural behavior of SFRC beam was observed in three stages.

The first stage is linear behavior of loading and deflection relationship until the tensile stress reaches the concrete tensile strength at first cracking point. After that, the stiffness reduces with load increasing beyond the first cracking load until yielding load stage.

The second stage is load after yielding point where the tensile steel is yield and cracks are significantly increasing. During this stage the second change of stiffness was significantly observed, and crack opens wider with the slight load increasing. From the experiment, with increasing the fiber content in SFRC beams has higher yielding load compared to RC beam.

The last stage is the ultimate loading strength until load decreasing (the failure of the beams). In this stage, the load slightly increases after yielding stage until the beam reaches the maximum load resistance at a certain deflection. The load deflection curve explains that RC beam experiences sudden failure after reaching the ultimate load, while SFRC beams resist the load significantly longer until the failure. This can confirm the bridging mechanism of steel fiber across the cracks that carries out more stress transfer. From the four-point bending test, all specimens failed in the flexural failure where the cracks were crushed on the top of the beam and many other cracks were formed on the compression zone of specimens. Fig. 15 shows the crack pattern after loading test of C19F1.5.

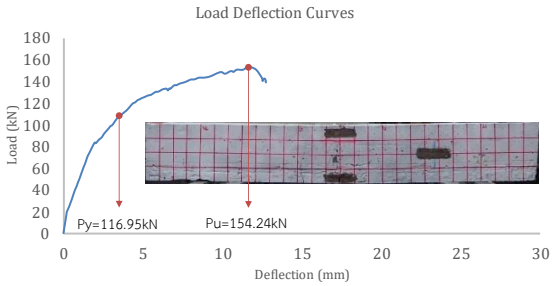

Fig. 11 Load displacement of C19F0 beam

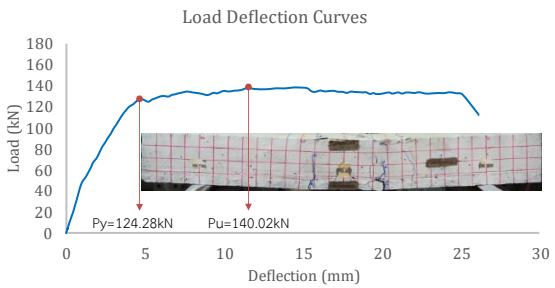

Fig. 12 Load displacement of C19F0.5 beam.

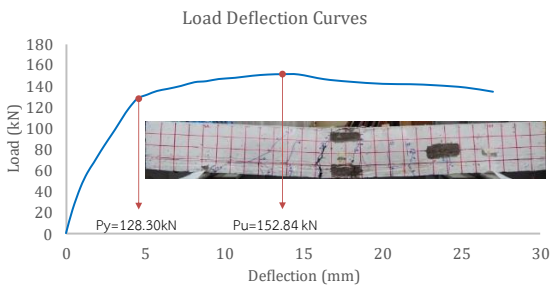

Fig. 13 Load displacement of C19F1.0 beam

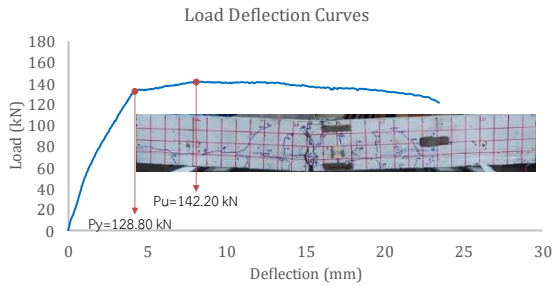

Fig. 14 Load displacement of C19F1.5 beam.

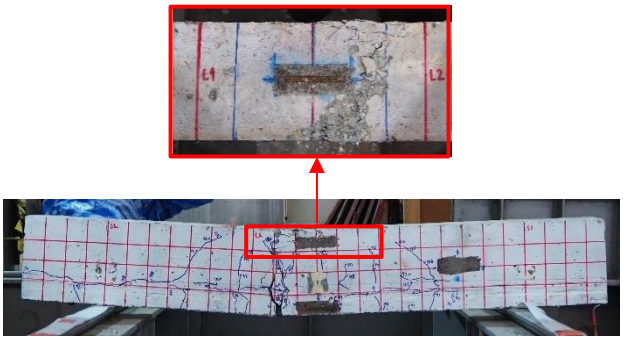

Fig. 15 Crack patter after loading of beam C19F1.5

3.3 Flexural performance and crack relation

Table 4 summarizes the loading at yield and ultimate load stages. At yield stage, RC beam presented the lowest yielding load as 116.95 kN, while the C19F1.5 had the highest yield of 128.80 kN. Moreover, with higher amount of fiber volume in the beam, it affected the improvement of yielding load as the increase of 6%, 9%, and 9% for the beam C19F5, C19F10 and C19F15 compared to the RC beam, respectively.

At ultimate stage, the increasing of steel fiber improved the flexural capacity significantly from 140.02 kN for C19F0.5 to the maximum of 152.84 kN for C19F1.0. However, the loading capacity of C19F0 was higher than the others even if there was not the steel fiber inside. This curious situation can be confirmed when the exact amount of corrosion in rebars will be investigated. In addition, by considering the yielding load and the maximum capacity of C19F1.5, it showed unusual results even it was the beam with highest amount of fiber because the error of corrosion inducing was found in one longitudinal steel bar. Therefore, it has the possibility that all the current may induce to the other bar during the acceleration process and cause early failure.

Table 4 Flexural bending test result.

Beams	Yield Stage		Ultimate Stage	
	Load (kN)	Deflection (mm)	Load (kN)	Deflection (mm)
C19F0	116.95	4.32	154.24	11.74
C19F0.5	124.28	4.48	140.02	11.77
C19F1.0	128.30	4.08	152.84	13.91
C19F1.5	128.80	3.77	142.20	8.52

Eventually, the effect of steel fiber plays an important role in flexural bending behavior of the beam. Even though specimen C19F0 reached the maximum load at 154.24 kN but it experienced sudden failure due to the absence of steel fiber. Meanwhile, the specimen C19F0.5, C19F1.0 and C19F1.5 resisted the much longer deflection with stable load resisting than C19F0 although the load was beyond yielding stage. This high improvement in ductility of corroded beams indicates the bridging mechanism of steel fibers that significantly restrains the crack. As a result, more stress can transfer through the restrained crack and induces greater load resistance.

4. Conclusions

This study provided the effect of various amounts of steel fibers on crack propagation and flexural behavior of the corrosive beams. Flexural bending test was conducted to obtain the flexural strength and failure pattern of the corrosive beams. Based on the experimental data, the conclusions can be drawn as follows:

1. The use of steel fiber greatly reduced the cracks in beam C19F0, C19F0.5, C19F1.0 and C19F1.5 by 0.23mm, 0.21mm, 0.19mm and 0.17mm respectively. Moreover, by adding higher amount of steel fiber, the crack propagation in the SFRC beam develops slower than RC beam.
2. The yield and ultimate load capacity of SFRC beams significantly increase with the rising volume of steel fiber. The yield capacity of beams C19F0.5, C19F1.0, and C19F1.5 increased by 6%, 9%, and 9% compared to RC beam, respectively.
3. Steel fiber significantly contributes ductile behavior of the beams and maintains the stable load resistance although beyond the yielding load stage.

References

[1] Broomfield, J. P. (2023). *Corrosion of steel in concrete: understanding, investigation and repair*. Crc Press., pp. 18

[2] Carvalho, M. R., Barros, J. A., Zhang, Y., & Dias-da-Costa, D. (2020). A computational model for simulation of steel fibre reinforced concrete with explicit fibres and cracks. *Computer Methods in Applied Mechanics and Engineering*, *363*, 112879.

[3] Vo, K. M., Pansuk, W., Cao, T. N., & Nguyen, H. Y. T. (2023). Flexural Performance of Mill Cut Steel Fiber Reinforced Concrete Beam Degraded by Mild Corrosion. Proceedings of The 17th East Asian-Pacific Conference on Structural Engineering and Construction, 2022: EASEC-17, Singapore,

[4] Frazão, C., Díaz, B., Barros, J., Bogas, J. A., & Toptan, F. (2019). An experimental study on the corrosion susceptibility of Recycled Steel Fiber Reinforced Concrete. *Cement and Concrete Composites*, 96, pp.138-153.

[5] Olivito, R., & Zuccarello, F. (2010). An experimental study on the tensile strength of steel fiber reinforced concrete. *Composites Part B: Engineering*, 41(3), pp.246-255.

[6] Hou, L., Zhou, B., Guo, S., Zhuang, N., & Chen, D. (2018). Bond-slip behavior between pre-corroded rebar and steel fiber reinforced concrete. *Construction and Building Materials*, 182, pp.637-645.

[7] Pyo, S., Koh, T., Tafesse, M., & Kim, H.-K. (2019). Chloride-induced corrosion of steel fiber near the surface of ultra-high performance concrete and its effect on flexural behavior with various thickness. *Construction and Building Materials*, 224, pp.206-213.

[8] Mak, M. W., Desnerck, P., & Lees, J. (2018). Correlation between surface crack width and steel corrosion in reinforced concrete.

[9] Song, J., Nguyen, D. L., Manathamsombat, C., & Kim, D. J. (2015). Effect of fiber volume content on electromechanical behavior of strain-hardening steel-fiber-reinforced cementitious composites. *Journal of Composite Materials*, 49(29), pp.3621-3634.

[10] Hou, L., Ye, Z., Zhou, B., Shen, C., Aslani, F., & Chen, D. (2019). Bond behavior of reinforcement embedded in steel fiber reinforced concrete under chloride attack. *Structural Concrete*, 20(6), pp.2242-2255.

[11] Committee, A. (2019). Building code requirements for structural concrete (ACI 318-19) and commentary.

[12] Spainhour, L. K., & Wootton, I. A. (2008). Corrosion process and abatement in reinforced concrete wrapped by fiber reinforced polymer. *Cement and Concrete Composites*, 30(6), pp.535-543.

[13] Morshed, A. Z., Shakib, S., & Jahin, T. (2020). Characterization of Impressed Current Technique to Model Corrosion of Reinforcement in Concrete. *Journal of Engineering Science*, 11(1), pp.93-99.